Composites: Part B 42 (2011) 949–961

Contents lists available at ScienceDirect

Composites: Part B

journal homepage: www.elsevier.com/locate/compositesb

Mechanically fastened joints in composite laminates: Evaluation of load bearing capacity

A.A. Pisano, P. Fuschi *

Dipartimento Arte Scienza e Tecnica del Costruire, University Mediterranea of Reggio Calabria, via Melissari, I-89124 Reggio Calabria, Italy

ARTICLE INFO

Article history:
Received 23 March 2010
Received in revised form 18 December 2010
Accepted 22 December 2010
Available online 31 December 2010

Keywords:
A. Laminates
B. Strength
C. Numerical analysis

ABSTRACT

Mechanical fasteners, commonly used in many advanced engineering applications dealing with composite laminates, play the main role of transferring loads between the linked structural elements. The present study, focused on pinned-joints, explores the possibility of applying a *direct method* for evaluating the joint's strength as well as for predicting some of the more common joint's failure mechanisms. A *limit analysis numerical approach* for statically loaded pinned-joint orthotropic laminates in plane stress conditions is proposed. Two well known numerical procedures for limit analysis likewise having common roots, namely the Linear Matching Method and the Elastic Compensation Method, are utilized to evaluate upper and lower bounds to the joint collapse load. Both methods are rephrased assuming for the material in use a Tsai–Wu type yield surface. The results obtained are compared and plotted against some available experimental findings. Some final remarks draw attention to the potentialities and the limits of the proposed approach.

1. Introduction

Mechanical properties of composite laminates, nowadays widely employed in many advanced engineering fields, make them attractive for structural applications where high strength-to-weight and stiffness-to-weight ratios are required. Mechanical fasteners (like bolts, rivets, pin-connectors) are commonly used in these applications for transferring loads between the structural components. Such fasteners, extensively used mainly because they are easy to assemble or disassemble, are characterized by an high stress concentration near the hole area which becomes a source of weakness; the structural joint failure usually beginning at the fasteners sites. A great deal of research has therefore concentrated on the evaluation of the joint's strength as well as on the prediction of the failure mechanism. The review papers of Camanho and Matthews [10] and Thoppul et al. [57] provide an extensive list of pertinent contributions covering the past two decades, some of which also dealing with the current design practice for pinned-joints and connections. Undoubtedly, the bright and actual interest on this research subject is witnessed by very recent contributions, see e.g. Ascione et al. [3,4] or Gray and McCarthy [23].

Analytical (continuum approaches) and numerical (mainly finite element based approaches) methods have been used to perform *stress analyses* on mechanically fastened joints. Following this research line the main task is the deduction of the *stress distribution around the fastener hole*. To this aim different hypotheses are assumed on the pin-hole interaction concerning, for example, the modelling of the pin, the load distribution at the pin-hole boundary, the stacking sequence of the laminate and so all the through-thickness effects like, for example, friction or clearances. In particular, the analytical methods are mainly based on orthotropic elasticity problems formulated in terms of complex variable theory, the numerical methods are grounded on two-dimensional finite element analyses in conjunction with classical lamination theory. Iterative or inverse methods have been also used in this context, as well as many three-dimensional finite element models have been proposed to take into account through-thickness effects.

A considerable number of approaches are also those based on the *strength prediction methods*. The determination of the joint strength depends on the definition of failure that can vary from the maximum load sustained by the joint to a criterion based on the deformation of the hole. Failure theories at the lamina level or point- and average-stress methods, the latter taking into account localized damage, belong to this second research line. In the same context can be also framed the methods based on linear elastic fracture mechanics and the progressive damage models. The latter, developed to deal with the damage that occurs prior to laminate failure, try to simulate damage initiation and growth using elastic property degradation models.

A third, more recent, research line includes experimental studies, mechanical test standards and, in general, *semi-empirical procedures combined with experimental data* to predict the joint strength as a function of the basic laminate properties and joint geometrical

* Corresponding author. Tel.: +39 0965 3223140; fax: +39 0965 21158.
E-mail address: paolo.fuschi@unirc.it (P. Fuschi).

1359-8368/$ - see front matter © 2010 Elsevier Ltd. All rights reserved.
doi:10.1016/j.compositesb.2010.12.016

parameters. A variety of recent joint design methodologies involve numerical analyses either based on finite (or boundary) element codes or even on genetic algorithms. The significant advances that have been made in the experimental characterization of the joint failure modes through non-destructive evaluation techniques allowed the use of the above approaches often related to an accurate identification of material parameters.

As general remark it is worth to note that a common requisite of the different approaches, aimed at analyze mechanically fastened joints, is the knowledge of the experimental joint behaviour either in terms of modes of failure or in terms of influence the geometric and material parameters have on its mechanical response. The through-thickness effects or the environmental conditions affecting the mechanical properties of the constituent materials are other important matters that should be taken into account.

In the present study, far off the will of furnishing an exhaustive solution to such a complex problem, a *limit analysis numerical approach* for statically loaded pinned-joint orthotropic laminates in plane stress conditions is proposed. The same problem has been treated, in terms of evaluation of an upper bound to the collapse load multiplier, in a very recent contribution of the present authors [22]. The results there presented, although confirming the potentialities of the approach, either in terms of estimation of the collapse load value or in terms of collapse mode prediction, are affected by the congenital inability of a method based on the kinematic approach of limit analysis applied to a *non standard* material; namely the inability of predicting how far is the computed upper bound from the real collapse load value. As known, the general lack of associativity of an anisotropic composite material, even if can be handled by a nonstandard limit analysis approach, see e.g. Lubliner [34], Radenkovic [46], generates an unavoidable gap between the upper bound and the collapse load value whose knowledge is nevertheless essential for practical engineering applications.

In this context a crucial task for design purposes is indeed the definition of a lower bound to the collapse load multiplier and the consequent assessment of the gap between the two bounds, namely the upper and lower one; this is one of the main goal of the present study. The comparison between the obtained numerical results and the experimental ones, available for the chosen mechanical problem, is another essential task of the present study being aware of the fact that there is no definitive method to predict joint strength but as much aware that the effectiveness of a numerical method can be judged only by comparison with experimental findings.

The proposed numerical approach, refer to Fuschi et al. [22] and Pisano and Fuschi [42] for its kinematic version, can be viewed as an extension, in the context of orthotropic materials, of a method known in the relevant literature as *Linear Matching Method* (LMM), see e.g. Ponter and Carter [43]; Ponter et al. [44]; Chen et al. [14]; Barrera et al. [6]. The LMM turns to an iterative procedure providing, at each iteration, an upper and a lower bound to the collapse load. In practice the obtained lower bound is a lower bound to the least upper bound of the computed sequence and, in this sense, it can be viewed as a *pseudo* lower bound (Ponter and Carter [43]). The evaluation of the lower bound is then also carried on following the procedure applied in Mackenzie and Boyle [36], and recently extended in Hamilton and Boyle [24], known as *Elastic Compensation Method* (ECM). The latter method, proposed in the early nineties, is actually the precursor of the LMM, both methods sharing many common characteristics. The two methods are rephrased and adapted to the assumed constitutive laws and the differences obtained in terms of lower bounds evaluation are outlined for the run examples.

The examined structural elements are composite laminates obeying, *by hypothesis*, to a *Tsai–Wu type yield criterion* defined as a second-order tensor polynomial form of the Tsai–Wu failure criterion for composite laminates [59]. This criterion is one of the best known showing a very good capability for predicting failure of composite laminates [56].

A few numerical examples are carried out to verify the effectiveness of the proposed approach as well as to inquire into its capability to predict experimental test results for pinned-joint composite prototypes. The numerically detected upper and lower bounds to the collapse load allows one to predict a range of limit load values within which the real collapse load should be located. Precisely, four experimental laboratory tests (after [61]) have been chosen as cases-study; they actually exhibit the typical different collapse joint mechanisms. The numerical results, obtained in terms of collapse mode prediction of the analyzed prototypes, are indeed very encouraging either for the very good agreement with the experimental findings or for the ability of the proposed procedure to locate accurately the collapse zone and the related collapse mode.

The structure of the paper is the following: after this introductory section, Section 2 poses the mechanical problem, i.e. a pin-loaded plate in tension, and frames the basic concepts and assumptions for its treatment via a limit analysis approach. Section 3 summarizes some basic concepts of limit analysis theory focusing on its application to non standard materials. The constitutive assumptions are also stated. An abridged description of the LMM and the techniques for the numerical evaluation of an upper and a lower bound on the collapse load are given in Section 4. The differences in the lower bounds evaluation via the LMM and the ECM are then investigated and pointed out at closure of this section. All the numerical findings are given in Section 5 where the potentialities and the limits of the proposed approach are outlined. Some final remarks together with critical comments and possible improvements are finally given in Section 6 which closes the paper.

1.1. Notation

Subscripts denote Cartesian components and the repeated index summation rule is to be applied. Bold face symbols denote vectors or tensors. Cartesian orthogonal co-ordinates $\boldsymbol{x} = (x_1, x_2, x_3)$ are employed. The symbol := means equality by definition. Other symbols will be defined in the text where they appear for the first time.

2. The mechanical problem: a pinned-joint composite plate

Let us consider the pin loaded rectangular composite plate of Fig. 1 where the fixture test for load bearing capacity evaluation as well as the geometry, boundary and loading conditions of the pertinent mechanical model are sketched. The plate has: length

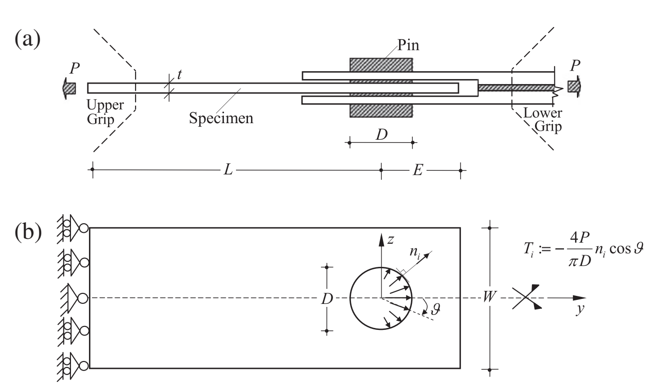

Fig. 1. Schematic representation of a pin-loaded composite rectangular plate: (a) fixture test for load bearing capacity evaluation; (b) mechanical model, boundary and loading conditions.

$L + E$; width W; thickness t; the fastener hole has diameter D and is located on the symmetry axes of the plate (y) at a distance E from the free edge. The pin is assumed rigid and located at the centre of the fastener hole. The loading is modelled as a load P transmitted by the pin to the plate being the upper grip edge the external constrained boundary. The further hypothesis of a cosine load normal distribution to approximate the pressure exerted by the pin on the inner hole surface is here assumed. To this concern, with reference to Fig. 1b, T_i denote the acting normal loads, n_i the unit vector normal to the inner hole surface and θ a clockwise angle varying in the range $[-\pi/2, \pi/2]$. It is worth noting that such a cosinusoidal stress distribution was found by several authors to be satisfactorily accurate only for quasi-isotropic laminates and small clearances. The scheme of Fig. 1 is then the typical one to study mechanically fastened pinned or bolted joints in composite laminate, attention is hereafter focused on pinned-joints.

As observed in the relevant literature, see e.g. the review papers of Camanho and Matthews [10], Thoppul et al. [57] and references therein, the joints are often the critical part of a composite structure and the main research efforts are oriented to comprehend all the aspects of the joint design. As suggested in Camanho and Lambert [9] a reliable methodology to design mechanically fastened joints in composite laminates has to be able to predict both the *elastic limit* of the joint, i.e. the load at which crack initiation takes place, and the *ultimate failure load* of the joint. The capability to detect the *failure modes* of the joint should also be assured. Typically, three main failure modes can be individuated, see e.g. Fig. 2a–c, other modes being a combination of them or, simply, secondary modes, see e.g. Fig. 2d and e; see again Thoppul et al. [57] or D5961/D5961M-05 Standards [17]. Concerning the main failure modes, it is known that net tension and shear out are catastrophic and due to excessive tensile stress value on the net area through the fastener hole and excessive shear stress on the areas emanating from the hole edge parallel to the load, respectively. Net tension and shear out modes can be avoided by increasing the ratios W/D or E/W respectively. Bearing failure is characterized by high

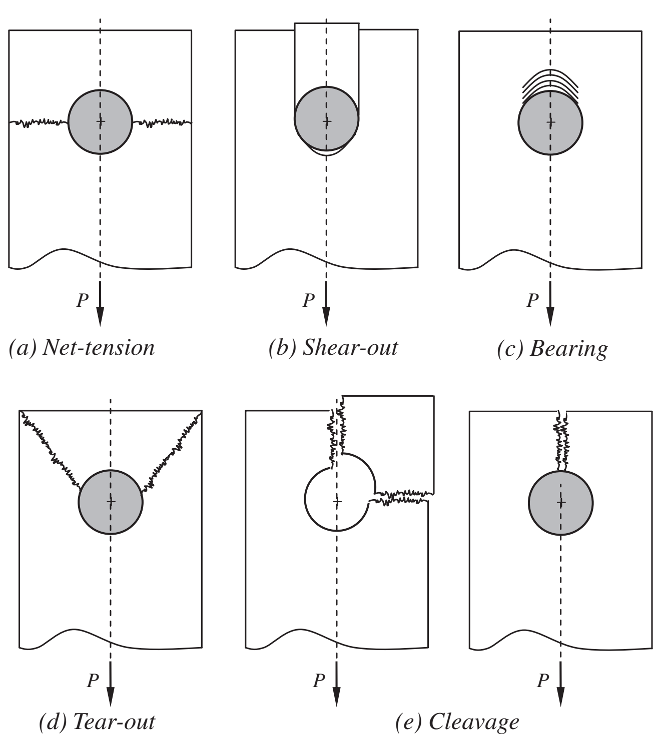

Fig. 2. Pin-loaded rectangular plate: sketch of the typical failure modes.

compressive stress values within the zone surrounding the loaded inner hole surface and it is a gradual and progressive failure mode of non-catastrophic nature. Secondary failure modes, such as tear out and cleavage, occur only after bearing failure and are not considered in the following.

Even if the posed problem has been deeply studied since the late seventies, many questions are still open to discussion. It is known that the failure of a mechanically fastened joint depends on many factors, e.g. connection geometry; constituent materials properties; fiber orientation; stacking sequence; position of the fastener hole; clearance; loading conditions; or, for composite having polymeric constituents, environmental conditions. For polymer–matrix composites, for example, creep, relaxation and other manifestations of viscoelastic behaviour exhibited at room temperature can be magnified at elevated moisture and/or temperature levels. Aging can also affect the mechanical properties of the constituent materials. The list of factors is certainly not complete and, obviously, even sophisticated joint design methodologies, involving the use of computer-based methods fed by experimentally identified material parameters, cannot handle the complexity of the problem. Many approaches result often very effective and precise only for specific joint set up and specific composite laminates being indeed hardly generalizable to other contexts or materials.

The *limit analysis numerical method* here proposed tackles the pinned-joint problem at a (macro) *structural level*. The method is focused on the possibility of locating a range of load levels bracketing the load value which produces the joint collapse. It might be from many aspects inaccurate but, with all its limits and approximations discussed in the following, it appears simple, rather effective, of general applicability, being also able to catch some important aspects of the overall joint behaviour at collapse.

Three main simplifying assumptions are adopted to analyze the pinned-joint problem: (i) the effects of the actual stacking sequence of the laminate are not taken into account and an equivalent single layer laminate is analyzed, i.e. an homogenization process is implicitly assumed; (ii) three-dimensional or, through-thickness effects are neglected and a plane stress problem is considered; (iii) the constitutive behaviour of the composite laminate obeys, by hypothesis, to a second-order tensor polynomial form of Tsai-Hu failure criterion (Tsai and Wu [59]). Other simplifying assumptions concerning the limit analysis theory in the context of non standard materials are given in the next Section where the fundamentals of the LMM, extended by the authors to orthotropic materials in Fuschi et al. [22], are briefly summarized.

3. Limit analysis for orthotropic laminates

Limit analysis allows the direct evaluation of the load bearing capacity of a structure or of a structural element. In its classical (original) formulation the theory of limit analysis refers to perfectly plastic structures and it is based on a lower and an upper bound theorem (Drucker et al. [19]; Prager [45]). The bound theorems allow the exact determination of the load value that will cause collapse.

Following a standard formalism, an upper bound to the collapse load multiplier for a given body of volume V is given by:

$$P_{UB} \int_{\partial V_t} \bar{p}_i \dot{u}_i^c \, \mathrm{d}(\partial V) = \int_V \sigma_j^Y \dot{\varepsilon}_j^c \, \mathrm{d}V, \tag{1}$$

where $\dot{\varepsilon}_j^c = \dot{\lambda}\partial f/\partial\sigma_j$ are the components of the strain rate at collapse having the direction of the outward normal to the yield surface $f(\sigma_j) = 0$ (with $\dot{\lambda} > 0$ a scalar multiplier); σ_j^Y are the stresses at yield associated to the given compatible strain rates $\dot{\varepsilon}_j^c$; $\dot{u}_i^c$ are the related displacement rates. Moreover, $\bar{p}_i$ are the surface force components of the reference load vector $\bar{\mathbf{p}}$ acting on the external portion ∂V_t

of the body surface. For simplicity, only surface forces are considered. Finally, P_{UB} denotes the upper bound load multiplier. The set $(\dot{\varepsilon}_j^c, \dot{u}_i^c)$ defines a collapse mechanism. On the other hand, if at every point within V exists a stress field $\tilde{\sigma}_j$ which satisfies the condition $f(\tilde{\sigma}_j) \leqslant 0$ and in equilibrium with the applied load $P\bar{\mathbf{p}}$ for a value of P, say P_{LB}, then P_{LB} is a lower bound to the collapse limit load multiplier. The two assertions above, as known, lead to two classical approaches of limit analysis, namely: the kinematic and the static one. If the loads produced by their application are equal to each other, circumstance verifiable only for standard materials, then they equal the collapse load.

The rapid development of finite element based analyses was undoubtedly an essential contribution to the success of direct methods (see e.g. Hodge and Belytschko [27]; Belytschko and Hodge [7]; Save [47]; Chen and Shu [15]). Linear programming first (see e.g. Sloan [54]), nonlinear programming algorithms after (see e.g. Lyamin and Sloan [33]), till highly specialized optimization algorithm (see e.g. Andersen et al. [2]) are all examples of limit analysis approaches based on FE analyses in conjunction with optimization algorithms. The papers by Makrodimopoulos and Martin [37] or by Muñoz et al. [40], where second-order cone programming is applied to cohesive-frictional materials or within an adaptive remeshing strategy respectively, are, among other, the more recent contributions belonging to this research line. Limit analysis numerical approaches grounding on complex method, to solve nonlinear programming problem, in conjunction with symmetric Galerkin boundary element method or element-free Galerkin method (see e.g. Zhang et al. [64]; Chen et al. [12]) are other interesting examples of current research activity. For an updated review of the existing methodologies of the so-called "Direct Methods", embracing limit and shakedown analysis, with extensions to new horizons of application for industrial design, reference can be made to the very recent book of Weichert and Ponter [60].

Application of limit analysis outside the realm of perfect plasticity is witnessed by several studies even coeval of the pioneer ones like the papers by Drucker and Prager [20], Shield [52], Kooharian [30], Heyman [26], or, later on the studies of Radenkovic [46], Josselin de Jong [29], Palmer [41], Atkinson and Potts [5], till, among the more recent ones, the works of Sloan and Kleeman [55], Yu and Sloan [62], Zheng et al. [65], Boulbibane and Ponter [8]. Moreover, several studies (Shu and Rosen [53]; McLaughlin and Batterman [39], Francescato and Pastor [21]; Capsoni et al. [11]; Ma et al. [35]; Corradi and Vena [16]; Li and Yu [31]; Zhang et al. [63]) concern limit analysis in the context of composite laminates, some of them explicitly referring to orthotropic materials, i.e. the ones of interest in the present study. In this context has to be framed the methodology here adopted which follows a *nonstandard limit analysis theory* in the sense of Radenkovic (Lubliner [34]; Radenkovic [46]).

3.1. Non standard limit analysis and constitutive assumptions

Adopting Radenkovic's approach the two limit analysis fundamental theorems can be rephrased once again in the shape of upper and lower bound theorems, see e.g. Lubliner [34]. After all, *every value of the limit load for a non standard body is located between two fixed boundaries defined by the values of the limit loads computed considering the body made by two standard materials whose yield surfaces are one outer, the other inner, to that of the nonstandard material.* Obviously, Radenkovic's approach locates a range of collapse load multiplier values, because for non standard material structures the uniqueness of the limit load is uncertain.

Assuming for the material in use an *yield surface* expressed by a second-order tensor polynomial form of the Tsai–Wu criterion (Tsai and Wu [59]; Capsoni et al. [11]; Tsai and Hann [58]), the lack of associativity, if this latter essential requisite it is not postulated, may be overcome by the Radenkovic's approach.

By denoting with 1 and 2 the principal directions of orthotropy in plane stress case as well as indicating $\sigma_6 \equiv \tau_{12}$, as usual for composite laminates (see e.g. Jones [28]), the adopted Tsai–Wu type criterion is expressed by:

$$F_{11}\sigma_1^2 + F_{22}\sigma_2^2 + F_{66}\sigma_6^2 + 2F_{12}\sigma_1\sigma_2 + F_1\sigma_1 + F_2\sigma_2 = 1, \tag{2}$$

where

$$\begin{aligned} &F_1 := \frac{1}{X_t} + \frac{1}{X_c}; \quad F_2 := \frac{1}{Y_t} + \frac{1}{Y_c}; \quad F_{11} := -\frac{1}{X_t X_c}; \\ &F_{22} := -\frac{1}{Y_t Y_c}; \quad F_{66} := \frac{1}{S^2}; \quad F_{12} := -\frac{1}{2}\sqrt{F_{11}F_{22}}; \end{aligned} \tag{3}$$

with X_t, X_c the longitudinal tensile and compressive strengths respectively; Y_t, Y_c the transverse tensile and compressive strengths respectively and S the longitudinal shear strength. It is worth to remind that, in a dimensionless stress space, say (X, Y, Z), the simplified second-order form (2) can be written as:

$$X^2 + Y^2 + Z^2 + 2f_{12}XY + f_1X + f_2Y = 1, \tag{4}$$

where

$$\begin{aligned} &X := \sqrt{F_{11}}\sigma_1; \quad Y := \sqrt{F_{22}}\sigma_2; \quad Z := \sqrt{F_{66}}\sigma_6; \\ &f_{12} := \frac{F_{12}}{\sqrt{F_{11}F_{22}}}; \quad f_1 := \frac{F_1}{\sqrt{F_{11}}}; \quad f_2 := \frac{F_2}{\sqrt{F_{22}}}. \end{aligned} \tag{5}$$

Moreover, in the dimensionless space (X, Y, Z), Eq. (4) individuates an *ellipsoid* whose major axis lies on $Z = 0$ plane and it is rotated by a counterclockwise angle of *45* degrees with respect to the X axis.

The choice of the Tsai–Wu failure criterion, as base to define an yield surface, grounds on the following remarks:

(i) The Tsai–Wu interactive failure criterion belongs to the five leading theories selected within the World-Wide-Failure-Exercise conceived to establish the current status of failure prediction theories for polymer composite laminates, as the ones treated hereafter (see e.g. Soden et al. [56] and references therein or the recent contribution of Lopez et al. [32]).

(ii) The Tsai–Wu type yield criterion, in the quadratic form adopted, is simple; it allows one to apply the standard rules of transformation, invariance and symmetry; it also contemplates interactions among the stress or strain components analogously to the Von Mises criterion for isotropic materials.

(iii) The adopted yield criterion is used to locate stress states at which the material has exhausted its strength capabilities, namely stress points lying on the domain boundary. The assumption of an yield surface in the shape given by Eqs. (2) or (4), is of axiomatic type and is necessary to perform limit analysis. To assume the further hypothesis of an associate flow rule is, at least in principle, possible but it does not seem appropriate for orthotropic composite materials. The choice to consider a non associate flow rule, so resorting to a nonstandard limit analysis approach, appears, to the Authors' opinion, more general and confers a wider applicability to the proposed procedure which can be easily implemented with different (convex) yield surfaces.

(iv) On taking into account both the strict convexity of the yield surface (2) or (4) and the Radenkovic's first statement, it will be possible to search for an upper bound on the collapse load multiplier with reference to the Tsai–Wu type surface itself. A different strategy, with respect to the Radenkovic's second statement, will be adopted for the lower bound evaluation which would require the knowledge of a plastic potential function for the non standard material in use. This point will be deeply discussed in the next section.

4. Limit analysis via FE-based numerical methods

4.1. Linear Matching Method for upper and lower bounds evaluation

The LMM, theorized and worked out by Ponter and co-workers in the last decade (see e.g. Ponter and Carter [43]; Ponter et al. [44]; Chen et al. [14]; Barrera et al. [6]), has been recently extended to orthotropic composite laminates by the present authors, Fuschi et al. [22]. The quoted papers are then referred to for a detailed description of the method; hereafter only a brief summary, aimed at highlight the essentials of the method, is reported. A major attention is indeed focused on the lower bound evaluation carried out within the expounded procedure.

On taking into account Eq. (1) and the formalism adopted at Section 3 for the evaluation of the bounds on the collapse load the following can be stated. The LMM is aimed at constructing a collapse mechanism—namely the kinematic fields $\dot{\varepsilon}^c_j$, $\dot{u}^c_i$—for the evaluation of a P_{UB} or, at defining an equilibrated stress distribution satisfying the admissibility conditions—namely $\tilde{\sigma}_j$—for the evaluation of a P_{LB}. Moreover, the LMM involves a *sequence* of FE-based analyses assuming the studied structure as made of a material with spatially varying moduli, i.e. a *fictitious material*. Let discuss the upper bound evaluation first.

At each step—namely at each FE analysis—a fictitious FE-solution is used to define, at the Gauss points of the adopted FE mesh, a collapse mechanism for the real structure in terms of stress at yield, σ^Y_j, plus related strain and displacement rates, namely $\left(\dot{\varepsilon}^c_j, \dot{u}^c_i\right)$. Looking at Eq. (1), these information allows one to evaluate an upper bound to the collapse load multiplier. The sequence (i.e. the iterative process) stops when the difference between two subsequent upper bound values becomes less than a fixed tolerance.

The LMM here adopted utilizes a *fictitious linear viscous material* which is *orthotropic* and *subjected to a distribution of imposed initial stresses*. Reference is made to an orthotropic laminate under plane stress conditions whose material parameters, Young moduli and Poisson's ratio, have been fixed, say to values: $E^{(0)}_1$, $E^{(0)}_2$, $E^{(0)}_6$, $\nu^{(0)}_{12}$, respectively. The structure is also subjected to a given distribution of initial stresses: $\bar{\sigma}^{(0)}_1$, $\bar{\sigma}^{(0)}_2$, $\bar{\sigma}^{(0)}_6$. The notation $(\cdot)^{(0)}$ refers to an initial arbitrary choice of the quantity $(\cdot)$. For this fictitious material the *complementary dissipation rate* can be written as:

$$W\left(\sigma_j, E^{(0)}_j, \nu^{(0)}_{12}, \bar{\sigma}^{(0)}_j\right) = \frac{1}{2}\left[\frac{\sigma_1^2}{E^{(0)}_1} + \frac{\sigma_2^2}{E^{(0)}_2} + \frac{\sigma_6^2}{E^{(0)}_6} - 2\nu^{(0)}_{12}\frac{\sigma_1\sigma_2}{E^{(0)}_2} + \right.$$
$$-2\left(\frac{\bar{\sigma}^{(0)}_1}{E^{(0)}_1} - \nu^{(0)}_{12}\frac{\bar{\sigma}^{(0)}_2}{E^{(0)}_2}\right)\sigma_1 - 2\left(\frac{\bar{\sigma}^{(0)}_2}{E^{(0)}_2} - \nu^{(0)}_{12}\frac{\bar{\sigma}^{(0)}_1}{E^{(0)}_2}\right)\sigma_2 - 2\frac{\bar{\sigma}^{(0)}_6}{E^{(0)}_6}\sigma_6$$
$$\left. + \frac{\bar{\sigma}^{(0)^2}_1}{E^{(0)}_1} + \frac{\bar{\sigma}^{(0)^2}_2}{E^{(0)}_2} + \frac{\bar{\sigma}^{(0)^2}_6}{E^{(0)}_6} - 2\nu^{(0)}_{12}\frac{\bar{\sigma}^{(0)}_1\bar{\sigma}^{(0)}_2}{E^{(0)}_2}\right], \tag{6}$$

where by hypothesis, the moduli $E^{(0)}_j$ $(j = 1, 2, 6)$ are allowed to assume different values at different points in the structure, i.e. they are *spatially varying*, (the initial choice can assume the same values at all points). For this fictitious material and at a fixed value of the load multiplier, say $P^{(0)}_{UB}$, a linear FE-analysis is performed on the whole structure to compute: the strain rates $\dot{\varepsilon}^e_j = \partial W(\sigma^e_j/\partial\sigma^e_j)$; the related stresses σ^e_j; the compatible displacement rates, $\dot{u}^e_i$, of the points at which surface loads act. The *fictitious kinematic solution* $\left(\dot{\varepsilon}^e_j, \dot{u}^e_i\right)$ so computed (operatively at each Gauss point of the adopted FE mesh), is then *forced to represent a collapse mechanism*, namely it is forced to identify with $\left(\dot{\varepsilon}^c_j, \dot{u}^c_i\right)$ of Eq. (1).

To this aim, referring to the 3D sketch of Fig. 3 where, as assumed, the fixed fictitious *initial* values of the elastic parameters and stresses are denoted by $(\cdot)^{(0)}$, on keeping $\dot{\varepsilon}^e_j$ fixed, it is sufficient to compute the stress at yield, say σ^Y_j, associated to $\dot{\varepsilon}^e_j$—so *assumed* as a given $\dot{\varepsilon}^c_j$—and to vary (to scale down in the sketch of Fig. 3) the fictitious moduli and initial stresses (values $(\cdot)^{(*)}$ in Fig. 3) so that σ^e_j coincides with σ^Y_j; the fictitous $\dot{u}^e_i$ so representing the compatible displacements $\dot{u}^c_i$ associated to $\dot{\varepsilon}^c_j$. Executing such operation at all Gauss points of the discretized structure, Eq. (1) can be used to compute a $P^{(*)}_{UB}$. The above rationale, from a geometrical point of view (see again Fig. 3), merely states that the complementary dissipation rate equipotential surface of the fictitious material, $W\left(\sigma_j, E^{(*)}_j, \nu^{(*)}_{12}, \bar{\sigma}^{(*)}_j\right) = \text{const.}$, *matches* the Tsai–Wu type surface

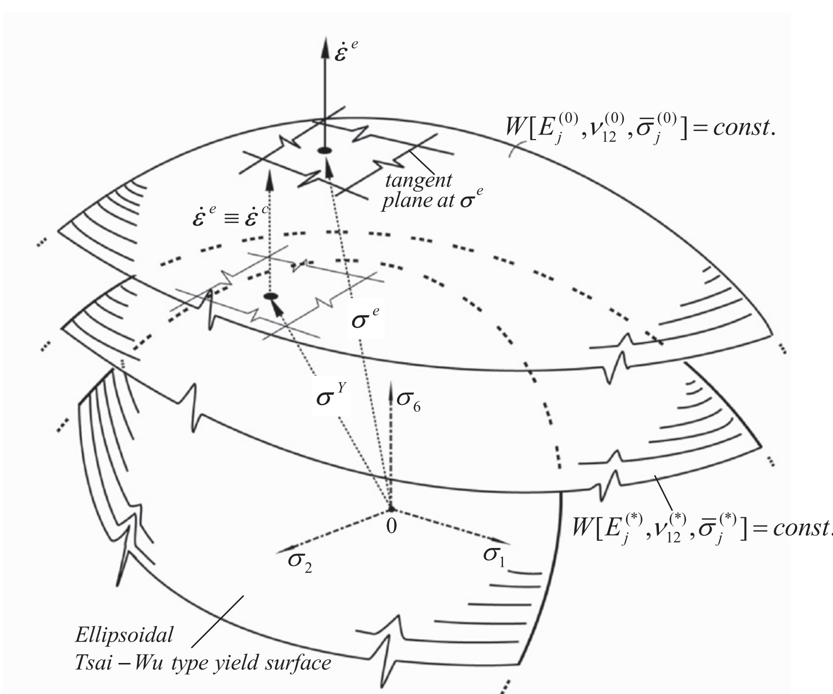

Fig. 3. 3D geometrical sketch, in the stress space (σ_1, σ_2, σ_6), of the matching procedure fulfilled at the generic Gauss point: $(\cdot)^{(0)}$ = initial arbitrary values; $(\cdot)^{(*)}$ = values at which the matching is achieved.

at the stress point σ_j^Y. The stresses at yield computed at matching, obviously do not satisfy the equilibrium conditions with the loads $P_{UB}^{(0)}\bar{\mathbf{p}}$ and a new fictitious analysis has to be performed on the whole structure with the updated $E_j^{(*)}$ values and loads $P_{UB}^{(*)}\bar{\mathbf{p}}$. Indeed, the whole procedure has to be carried out iteratively, the iterations stopping when two subsequent computed P_{UB} values become close to each other.

Remark 1. An essential requisite of an iterative procedure is the certainty of its convergence; to this concern, it is worth mentioning that the expounded procedure fulfils the sufficient condition for convergence given in Ponter et al. [44] and the final P_{UB} value is normally attained in few iterations.

Remark 2. The *formal analogy* existing between the linear viscous problem and the linear elastic problem allows one to compute, at each iteration, a *fictitious elastic solution*, looking at $W\left[\sigma_j, E_j^{(0)}, \nu_{12}^{(0)}, \bar{\sigma}_j^{(0)}\right]$ of Eq. (6) as at the complementary energy potential of a fictitious elastic material. The fictitious elastic analyses can then be carried out by any commercial FE-code with obvious advantages.

Remark 3. As noted in Ponter and Carter [43], the correctness of the P_{UB} depends on the kinematic description of the discretized problem and it is then related to the adopted FE mesh. In this sense the P_{UB} converges to the *minimum* upper bound *allowed* by the class of displacement fields given by the mesh itself. This drawback is easily overcome by using fine meshes in the analysis.

Remark 4. The matching, or the updating of the E_j values, is carried into effect at *each* GP in the FE mesh. However, to avoid accuracy problems, in a FE procedure a unique set of E_j—i.e. a unique (orthotropic) material—is assigned to each single element. To this aim, the $E_j^{(*)}$ updated at matching are averaged within the single element at the beginning of each FE analysis, the averaged values being given at all the GPs of the element.

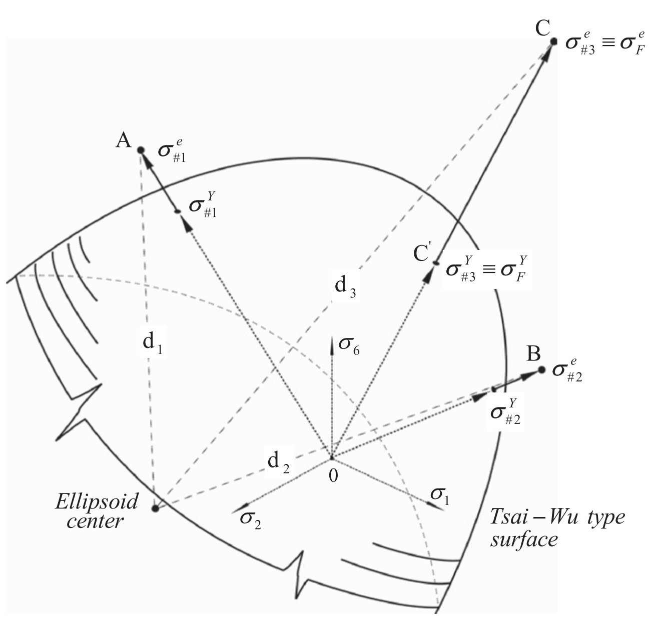

Fig. 4. 3D geometrical sketch, in the stress space $(\sigma_1, \sigma_2, \sigma_6)$, for lower bound evaluation: *A*, *B* and *C*, stress points representing the average stress values inside three generic FEs, say elements #1, #2 and #3; $\boldsymbol{\sigma}^e_{\#i}$ = average elastic stress within element #i (for P_{LB} evaluation $\boldsymbol{\sigma}^e_{\#i}$ it is also a *fictitious* stress); $\boldsymbol{\sigma}^Y_{\#i}$ = stress at yield on the direction $\boldsymbol{\sigma}^e_{\#i} / \mid \boldsymbol{\sigma}^e_{\#i} \mid$; d_i = distance of the stress point from the center of the Tsai–Wu type yield surface.

A lower bound, P_{LB}, to the collapse load multiplier can also be provided within the expounded procedure. At each iteration the *fictitious* stress values pertinent to loads $P_{UB}\bar{\mathbf{p}}$ and computed at each GP of each FE are averaged within the single element. It would be incorrect to average across elements since the elastic moduli of adjacent elements are different. A stress point corresponding to each averaged (element) value can then be located in the stress space. Among all such stress points the one farthest away from the Tsai–Wu type surface is detected, say $\boldsymbol{\sigma}_F^e$ (point *C* in Fig. 4) and this merely by computing the Euclidean distances from the ellipsoid center. The ratio ρ between the modulus of the yield stress vector measured on the direction $\boldsymbol{\sigma}_F^e / \mid \boldsymbol{\sigma}_F^e \mid$, say $\mid \boldsymbol{\sigma}_F^Y \mid$ (segment $\overline{OC'}$ in Fig. 4, where $d_3 > d_1 > d_2$), over the modulus of the stress vector $\mid \boldsymbol{\sigma}_F^e \mid$ (segment $\overline{OC}$ in Fig. 4) allows one to define a lower bound multiplier in the shape:

$$P_{LB} := \rho P_{UB} \quad \text{with} \quad \rho := \frac{\mid \boldsymbol{\sigma}_F^Y \mid}{\mid \boldsymbol{\sigma}_F^e \mid} < 1, \tag{7}$$

ρ being the rescaling factor such that all the computed stresses $\rho\boldsymbol{\sigma}^e$—in equilibrium with the loads $\rho P_{UB}\bar{\mathbf{p}}$—satisfy the admissibility conditions of the static approach for limit analysis. Some further remarks can now be drawn.

Remark 5. The rationale followed for the P_{LB} evaluation gives a lower bound to the computed minimum upper bound; Eq. (7) yields, in facts, a *pseudo-lower bound*. A different strategy, based on the elastic compensation method (see e.g. Hamilton and Boyle [24]), will be examined in the next subsection.

Remark 6. The matching procedure can be implemented in a much simpler way if both surfaces, the Tsai–Wu type one, given by Eq. (2) and the complementary dissipation equipotential surface of the fictitious material, expressed by Eq. (6) in the shape $W\left[\sigma_j, E_j^{(0)}, \nu_{12}^{(0)}, \bar{\sigma}_j^{(0)}\right] = \text{const.} = \overline{W}^{(0)}$, are rephrased in the dimensionless stress space usually adopted for the Tsai–Wu criterion (see e.g. Eq. (4) and positions (5)). Such a simplification is obtainable by taking advantage either of the *ellipsoidal shapes* of the two surfaces or of their *simpler analytical forms* in (X, Y, Z)-space. If the fictitious material is, from the beginning of the analysis, defined in such a way that its complementary energy equipotential surface is *homothetic* to the Tsai–Wu type surface, the two ellipsoids can be made coincident at matching. As a consequence, *only one* scalar *parameter* has to be iteratively updated, namely the *homothety ratio* between the two ellipsoids; see Fuschi et al. [22] for further details.

The whole iterative procedure is summarized in Table 1 for completeness.

4.2. Lower bound evaluation via Elastic Compensation Method

The elastic compensation method was originally presented for lower bound limit analysis of pressure vessels components, Mackenzie and Boyle [36]. An estimate of the limit load was there achieved by a *sequence of elastic finite element analyses* aimed at producing an effective admissible stress field for the lower bound theorem. The method was later derived and verified for upper bound limits and shakedown problems (see e.g. Hamilton et al. [25] and references therein). The key ideas of the ECM can be traced back to a technique known as the "reduced modulus method for stress categorisation in pressure vessels". Following this method, rather than perform inelastic analyses, the inelastic response was investigated by iterative elastic analysis in which highly loaded regions of the structure were systematically weakened by reduction of the local modulus of elasticity and this in order to simulate the effects of local inelasticity (see e.g. Dhalla and

Table 1
Iterative scheme of the LMM for P_{UB} and P_{LB} evaluation.

- *Initialization*
  Knowing the strength values of the orthotropic material (X_c; X_t; Y_c; Y_t; S); assign to all FEs an initial set of fictitious elastic parameters and initial stresses such that the complementary energy equipotential surface is homothetic to the Tsai–Wu type surface, i.e.:

$$E_1^{(0)} = 1/(2F_{11}); \quad E_2^{(0)} = 1/(2F_{22}); \quad E_6^{(0)} = 1/(2F_{66});$$
$$\nu_{12}^{(0)} = -f_{12}\sqrt{F_{11}}/\sqrt{F_{22}};$$
$$\bar{\sigma}_1^{(0)} = \alpha_{TW}/\sqrt{F_{11}}; \quad \bar{\sigma}_2^{(0)} = \beta_{TW}/\sqrt{F_{22}}; \quad \bar{\sigma}_6^{(0)} = 0;$$

α_{TW} and β_{TW} being the X, Y co-ordinates of the Tsai–Wu type ellipsoid centre, while F_{11}, F_{22} and F_{66} are functions of the strength values. Set also: $k = 1$, $P_{UB}^{(k-1)} = P_{UB}^{(0)} = 1$ (for $k = 1$, $P_{UB}^{(0)}$ can be any arbitrary value) and compute the constant $\Omega = 1 + \alpha_{TW}^2 + 2f_{12}\alpha_{TW}\beta_{TW} + \beta_{TW}^2$ for later use.

- *Start iterations*

step # **1**: perform a fictitious elastic analysis with elastic parameters $E_j^{(k-1)}$, $\nu_{12} = \nu_{12}^{(0)}$, initial stresses $\bar{\sigma}_j = \bar{\sigma}_j^{(0)}$ and with loads $P_{UB}^{(k-1)}\bar{p}_i$, computing a fictitious elastic solution at Gauss point level, namely: $\dot{\varepsilon}_j^{e(k-1)}$, $\dot{u}_i^{(k-1)}$, $\sigma_j^{e(k-1)}$.

step # **2**: compute the constant value of the complementary potential energy:

$$\overline{W}^{(k-1)} = \frac{1}{2}\sigma_j^{e(k-1)}\varepsilon_j^{e(k-1)}$$

step # **3**: compute the homothety ratio, namely

$$\Gamma^{(k-1)} = \begin{cases} \sqrt{\Omega/\overline{W}^{(0)}} & \text{for } k = 1 \\ \sqrt{\overline{W}^{(k-2)}/\overline{W}^{(k-1)}} & \text{for } k > 1 \end{cases}$$

step # **4**: evaluate stresses at yield:

$$\sigma_1^{Y(k-1)} = \left[1 - \Gamma^{(k-1)}\right]\frac{\alpha_{TW}}{\sqrt{F_{11}}} + \Gamma^{(k-1)}\sigma_1^{e(k-1)}$$
$$\sigma_2^{Y(k-1)} = \left[1 - \Gamma^{(k-1)}\right]\frac{\beta_{TW}}{\sqrt{F_{22}}} + \Gamma^{(k-1)}\sigma_2^{e(k-1)}$$
$$\sigma_6^{Y(k-1)} = \Gamma^{(k-1)}\sigma_6^{e(k-1)}$$

step # **5**: set $\dot{\varepsilon}_j^{c(k-1)} = \dot{\varepsilon}_j^{e(k-1)}$, $\dot{u}_i^{c(k-1)} = \dot{u}_i^{e(k-1)}$ and evaluate the upper bound multiplier

$$P_{UB}^{(k)} = \frac{\int_V \sigma_j^{Y(k-1)}\dot{\varepsilon}_j^{c(k-1)}\mathrm{d}V}{\int_{\partial V_t}\bar{p}_i\dot{u}_i^{c(k-1)}\mathrm{d}(\partial V)}$$

step # **6**: average the fictitious stress values inside each element and locate, among all the corresponding stress points, the one further away from the Tsai–Wu type surface, namely $\boldsymbol{\sigma}_F^{e(k-1)}$. Locate also the related stress point $\boldsymbol{\sigma}_F^{Y(k-1)}$ so computing the rescaling factor

$$\rho^{(k)} = \frac{|\boldsymbol{\sigma}_F^{Y(k-1)}|}{|\boldsymbol{\sigma}_F^{e(k-1)}|}$$

step # **7**: evaluate a lower bound multiplier

$$P_{LB}^{(k)} = \rho^{(k)}P_{UB}^{(k)}$$

step # **8**: check for convergence

$$|P_{UB}^{(k)} - P_{UB}^{(k-1)}| \leqslant \text{TOL} \quad \begin{cases} \text{YES} & \Rightarrow \quad \text{EXIT} \\ \text{NOT} & \Rightarrow \quad \text{CONTINUE} \end{cases}$$

step # **9**: compute the $E_j^{(k)}$ distribution accomplishing the matching at each GP to be utilized at next iteration, namely:

$$E_j^{(k)} = E_j^{(k-1)}[\Gamma^{(k-1)}]^2 \qquad j = 1, 2, 6$$

step # **10**: average the updated $E_j^{(k)}$ values within each element; set $k = k - 1$ and GOTO step #1

- *End iterations*

Jones [18], Marriot [38], Seshadri [48,49]). What is of interest in the above studies is obviously, rather than the actual categorisation, the way in which the effects of local inelasticity were assessed. And, in facts, in 1991 Seshadri and co-workers proposed a procedure for approximate estimates of limit load using the reduced modulus method (see e.g. Seshadri and Fernando [51], Seshadri [50]). The ECM hereafter employed refers to the paper of Mackenzie and Boyle [36] and to begin with a brief survey of the way it acts is given next.

A sequence of linear elastic FE analyses is carried out in which the elastic modulus in *each* element is modified, for the *i*th iteration, according to

$$E_{\#e}^{(i)} = E_{\#e}^{(i-1)}\frac{\sigma_n}{\sigma_{\#e}^{(i-1)}}, \tag{8}$$

where $E_{\#e}^{(i-1)}$ is the modulus used in the #*e*th element at previous analysis; σ_n is a "nominal" stress usually taken as half or two-thirds yield; $\sigma_{\#e}^{(i-1)}$ is the maximum unaveraged nodal *equivalent stress* attained within the *e*th element in the previous $(i-1)$ finite element solution. The procedure is carried out for a given arbitrary—perhaps the design—load level P_D until the maximum stress value in the whole FE mesh, measured in the *R*th iteration, has attained its lowest value, say σ_R, and is not reduced by further modifications of the elastic moduli. This near limit value σ_R, attained by the maximum stress in the model after several iterations, may or may not be smaller than the nominal yield stress of the material σ_Y. The iteration giving σ_R is, like all the other iterations, a linear elastic FE analysis and the computed value σ_R is proportional to the applied load P_D, i.e.

$$\sigma_R = \beta P_D, \tag{9}$$

βbeing the constant of proportionality evaluated at the *R*th (final) FE analysis. A lower bound on the limit load can then be estimated by simply observing that at the limit load level, say at load P_L, the maximum stress has just to reach the yield value σ_Y (at least in a region of the FE mesh) all the other stress values nowhere exceeding the yield stress. Such an admissible stress field for the load P_L, can then be generated from the final "compensated" *R*th FE elastic analysis if we set:

$$\sigma_Y = \beta P_L. \tag{10}$$

Rearranging and substituting for β by (9) gives:

$$P_L = \frac{\sigma_Y}{\beta} = \sigma_Y \frac{P_D}{\sigma_R}, \tag{11}$$

which corresponds to the highest load such that the final compensated stress in the elastic reduction procedure, σ_R, just reaches yield.

It is worth to note that, as suggested in Mackenzie and Boyle [36], the EC procedure can be applied only within "critical regions" identified by the elements with effective stress greater than the yield one, i.e. with $\sigma_{\#e} > \sigma_Y$. The elastic moduli within such elements is then adjusted according to:

$$E_{\#e}^{(i)} = E_{\#e}^{(i-1)} \frac{\sigma_Y}{\sigma_{\#e}^{(i-1)}}, \tag{12}$$

that is in proportion to the yield stress instead of the nominal stress as in Eq. (8). Another alternative concerns the value of the load P_D. The latter can be set assuming a value *above* that for the first yield, say P_Y; then the elastic moduli is corrected only for those FEs with effective stress above yield (i.e. with Eq. (12)), and the final iteration is the one at which the compensated elastically calculated stress σ_R just reaches (is below) the yield value σ_Y. The load is then increased and the reduction procedure repeated. Eventually further load increases will not allow compensated stresses to be brought below yield. The final admissible stress field corresponds to a given load level which is a lower bound on the limit load. This requires the compensation procedure to be applied incrementally in load, demanding more analyses, but with a better bound. In this context a simplified procedure which only requires analysis at one load level (50–80% above that for first yield P_Y) has been devised for torispherical pressure vessel heads in paper III of the trilogy by Mackenzie and Boyle [36].

An enhanced version of the ECM has been recently presented in Hamilton and Boyle [24] where the method is combined with a generalised yield criterion for lower bound limit analysis of transversely loaded thin plates. In this case a generalised plate yield surface of Ilyushin-type is assumed and Eqs. (8) and (11), used for the EC procedure and the estimation of the lower bound respectively, are rephrased in the shape:

$$E_{\#e}^{(i)} = E_{\#e}^{(i-1)} \frac{\sigma_n}{\Sigma_{\#e}^{(i-1)}}; \quad P_L = \sigma_Y \frac{P_D}{\Sigma_{max}}; \tag{13}$$

where $\Sigma_{\#e}^{(i-1)}$ is the yield function value evaluated for the (unaveraged) nodal stress resultant in element #*e*; Σ_{max} is the maximum yield function value in the FE plate model.

A modified ECM has been very recently proposed in Chen et al. [13] dealing whit structures containing flaws. A remarkable discussion on the convergence problem of the iterative ECM is firstly carried on employing Banach's contraction mapping theorem. A modified ECM is then proposed either to deal with local collapse modes or to avoid numerical singularities due to an over modification of the stiffness of elements whose stresses approach to zero.

As observed in Section 1, the ECM shares many common characteristics with the LMM being the ECM, from many aspects, the precursor of the LMM. The use of varying elastic moduli or the use of a sequence of elastic analyses (remember Remark 2 at Section 4.1) to mimic inelastic processes are, among other, common peculiarities of the two methods. However, to the authors' opinion, the two methods maintain their own originality and independence. The ECM is indeed strictly related to the concept of stress redistribution eventually aimed at producing an admissible stress field for the lower bound theorem. It then appears naturally oriented to a static approach of limit analysis. The LMM, also framable as a nonlinear programming technique (see e.g. Ponter and Carter [43], Barrera et al. [6]), is instead naturally related to the kinematic approach of limit analysis being able to construct a compatible collapse mechanism. Renouncing to examine and compare thoroughly the two methods, which is out of the scope of the present paper, but grounding on Remark 5 at Section 4.1, i.e. taking into account that the P_{LB} given by the LMM is actually a lower bound to the computed minimum upper bound, it is of interest to evaluate a lower bound also via the ECM. The latter approach is obviously reinterpreted on taking into account the improvements proposed in Hamilton and Boyle [24], Chen et al. [13] and it is "adapted" to the yield criterion here assumed for composite laminates in plane stress conditions.

Taking into account Eq. (12), the Young moduli of the #*e*th element, $E_{\#ej}$ (j = 1, 2, 6 for the orthotropic material in use), are updated only within selected zones, namely only within the FEs where $|\boldsymbol{\sigma}_{\#e}^{e}| > |\boldsymbol{\sigma}_{\#e}^{Y}|$. Differently from the previous formulae of the expounded ECM, reference is made to the moduli of the stress vectors in the stress space ($\sigma_1, \sigma_2, \sigma_6$). Referring again to Fig. 4, $\boldsymbol{\sigma}_{\#e}^{e}$ denotes the stress vector representing the average elastic stress value computed within the #*e*th element (his components are simply the averaged values of the stress components measured at the Gauss points of the element); $\boldsymbol{\sigma}_{\#e}^{Y}$ denotes the corresponding stress at yield measured on the direction $\boldsymbol{\sigma}_{\#e}^{e} / |\boldsymbol{\sigma}_{\#e}^{e}|$. Keeping the formalism of Eq. (12), the Young moduli within the #*e*th element (where $|\boldsymbol{\sigma}_{\#e}^{e}| > |\boldsymbol{\sigma}_{\#e}^{Y}|$) and at the ($i$)th elastic analysis are adjusted according to:

$$E_{\#ej}^{(i)} := E_{\#ej}^{(i-1)} \left[\frac{\left|\boldsymbol{\sigma}_{\#e}^{Y}\right|^{(i-1)}}{\left|\boldsymbol{\sigma}_{\#e}^{e}\right|^{(i-1)}} \right]^2, \tag{14}$$

where it is worth noting that the value of the stress at yield pertains to the current element and to the current elastic analysis while the square of the updating ratio is assumed to improve the convergence rate.

A lower bound to the collapse load multiplier is then computed via Eq. (11) with minor modifications, precisely by:

$$P_L := |\boldsymbol{\sigma}_R^{Y}| \frac{P_D}{|\boldsymbol{\sigma}_R|}, \tag{15}$$

where $\boldsymbol{\sigma}_R$ is the maximum stress detected in the whole mesh, $\boldsymbol{\sigma}_R^{Y}$ is the corresponding stress at yield (i.e. the stress lying on the Tsai–Wu type surface measured on the direction $\boldsymbol{\sigma}_R/|\boldsymbol{\sigma}_R|$); P_L and P_D are load multipliers of a unitary reference load *P*. The first sequence of elastic analyses is carried on with an arbitrary value of P_D, the moduli $E_{\#ej}$ are updated in *all* the FEs and $\boldsymbol{\sigma}_R$ is the lowest value attained in the mesh which is not reduced by further modifications of the elastic moduli. This first sequence produces a P_L of first tentative, say P_L'. A second sequence is then carried on with a $P_D > P_L'$, with elastic moduli updated *only* within the FEs where $|\boldsymbol{\sigma}_{\#e}^{e}| > |\boldsymbol{\sigma}_{\#e}^{Y}|$ and the final iteration (the R–th) is the one at which the compensated stress $\boldsymbol{\sigma}_R$ just reaches (is below) the yield value $\boldsymbol{\sigma}_R^{Y}$. Further sequences are then carried on with increased value of P_D and the reduction procedure repeated till further load increases do not allow the compensated stress $\boldsymbol{\sigma}_R$ to be brought below yield.

5. Estimation of the load bearing capacity of a pinned-joint

The LMM, in the shape given in Section 4.1, is applied to the mechanical problem posed in Section 2 (see also Fig. 1) to evaluate an upper and a lower bound to the collapse load multiplier. A lower bound evaluation is also carried out via the ECM in the shape stated at the end of Section 4.2. Reference is made to the work of Wu and Hahn [61], where several data and experimental results are reported for a pin-loaded plate in plane stress conditions.

The action of the pin inside the hole has been assumed, as explained in Section 2, as a cosine load normal distribution T_i (refer again to Fig. 1b). The plate, made of glass–fiber/vinyl–ester composite material fabricated by vacuum-assisted resin-transfer moulding, is indeed modelled as a symmetric quasi-isotropic laminate whose mechanical characteristics, in terms of strength values and elastic moduli, are reported in Table 2.

All the elastic analyses have been carried out using the commercial FE code Adina [1], while a Fortran main program has been developed to perform the iterative procedures either of the LMM or of the ECM. In the former method the Fortran code accomplishes also the matching at each Gauss point of each FE. Due to the symmetry of the problem with respect to the longitudinal axis, only one half of the plate has been analyzed using a FE mesh of the type shown in Fig. 5 with a total number of elements ranging between 350 and 550 isoparametric shell elements with 16 nodes and 16 GPs per element. The number of utilized FEs has been chosen depending on the geometry of the modelled test to obtain an accurate elastic FE solution; a finer mesh has been always employed around the fastener hole. Moreover, the utilized element allows to specify an orthogonal material axes system, the principal directions of orthotropy being $1 \equiv y$ and $2 \equiv z$. Finally, the applied reference load P has been assumed equal to 1 kN.

Table 2
Mechanical parameters of the composite laminate.

Elastic Moduli (GPa) and Poisson ratio	E_1 49.8	E_2 6.9	G_{12} 31.9	ν_{12} 0.3
Strengths (MPa)	$Y_t = X_t$ 664.3	$Y_c = X_c$ 385.1	S 64.6	

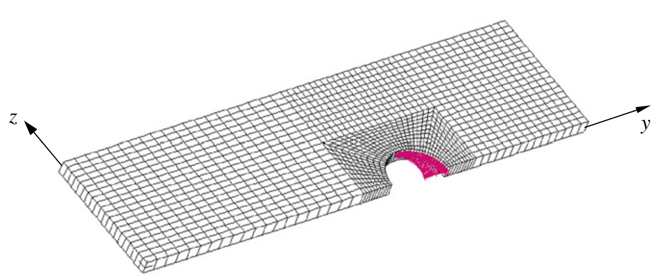

Fig. 5. Finite element model of the pin-loaded plate of Fig. 1: a number of (isoparametric 16 nodes/16 GPs) shell elements ranging between 350 and 550 has been adopted for the run tests to assure, for each test, an accurate elastic FE solution.

5.1. Numerical versus experimental findings: Validation

Among the experimental tests on different prototypes reported in Wu and Hahn [61] only four have been numerically reproduced. The chosen tests have been selected as cases-study exhibiting the typical collapse joint mechanisms. No significant further inquiry can be gained from numerical simulation of the whole set of laboratory tests given in the above quoted paper. In order to better understand the reliability of the proposed procedure additional simulations and analyses are undoubtedly necessary. A parametric analysis should be performed in order to investigate the influence of connection geometry, material properties, type of lamination (and consequent “homogeneization” performed) as well as the influence of testing procedure. A comparison with a step-by-step elasto-plastic analysis could be also useful. Nevertheless, to the Authors’ opinion, such analyses have to be performed on prototypes whose both manufacturing process and testing procedure are fully known. This is actually the object of an ongoing research program foreseing additional simulations and comparison with experimental, or numerical alternative, findings carried on prototypes manufactured and tested by the Authors. The present study is just a first attempt to apply a numerical limit analysis approach for the load bearing capacity evaluation of pinned joint connection in orthotropic laminates; the few experimental data get from the literature have then been chosen just to check the applicability of the proposed approach.

The obtained results are reported in Table 3 together with the experimental findings for sake of comparison. As said, the first three tests have been chosen mainly because they exhibit three different collapse mechanisms, the fourth one, together with the third one, is also useful to compare the performances of the LMM and the ECM for the lower bounds evaluation. The comparison between the experimental findings and the numerical predictions shown in Table 3 is made in terms of *ultimate bearing strength*, namely σ_{BRU}, defined as the “maximum stress reached before a reduction in stress occurs for the first time”. This bearing strength is given by the ratio between the load at failure, say P_f, and the product of the hole diameter times the plate thickness: $\sigma_{BRU} := P_f/(D \cdot t)$. Table 3 reports, for the considered specimens: the geometry; the experimental values of σ_{BRU} together with the experimentally observed failure mechanisms; the predicted σ_{BRU} values given by the present analysis via LMM and via ECM. In particular these latter (three) values have been computed *at last iteration* as: $P_{UB}P/(D \cdot t)$, $P_{LB}P/(D \cdot t)$ and $P_LP/(D \cdot t)$, respectively. The computed lower and upper bounds to the collapse load multiplier are also plotted against the experimentally detected collapse load multiplier in Figs. 6a and b and 7a and b versus the iteration number, each iteration corresponding to an elastic FE analysis of the plate.

By inspection of the obtained results, the ability of the proposed approach of bracketing the real collapse load value appears to be

Table 3
Pin-loaded plate of Fig. 1: experimental bearing strength values and failure modes against lower and upper bound predicted bearing strength values.

	Specimen dimensions				Experimental[a]		Prediction by LMM		Prediction by ECM
Specimen number	D (mm)	W/D	E/D	t (mm)	σ_{BRU} (MPa)	Failure mode	Upper σ_{BRU} (MPa)	Lower σ_{BRU} (MPa)	Lower σ_{BRU} (MPa)
1	6.35	4	6	2.32	496	T	520	387	302
2	6.35	8	4	2.27	522	B/S	518	443	315
3	6.35	8	6	2.28	439	B	532	516	286
4	12.70	4	3	1.15	281	B	385	362	209

[a] After Wu and Hahn [61].

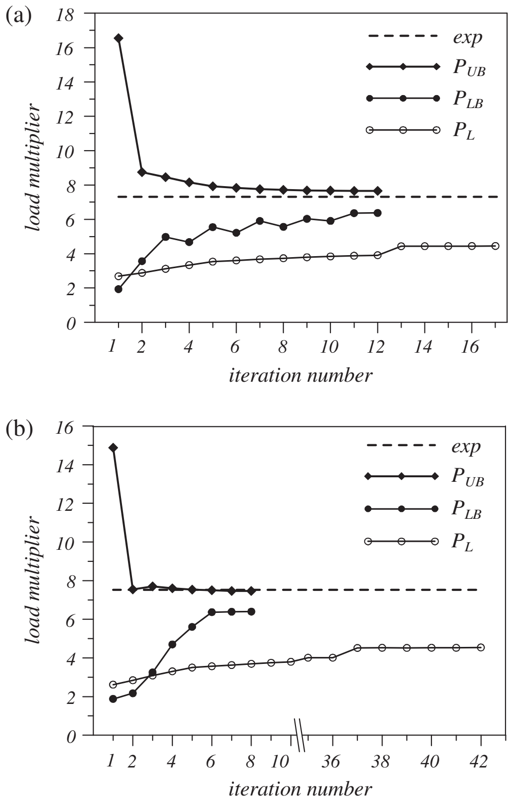

Fig. 6. Values of the upper (P_{UB}) and lower bounds (P_{LB} and P_L) to the collapse load multiplier versus iteration number; numerical results (solid lines with symbols) against collapse experimental treshold (dashed lines) for: (a) specimen #1; (b) specimen #2.

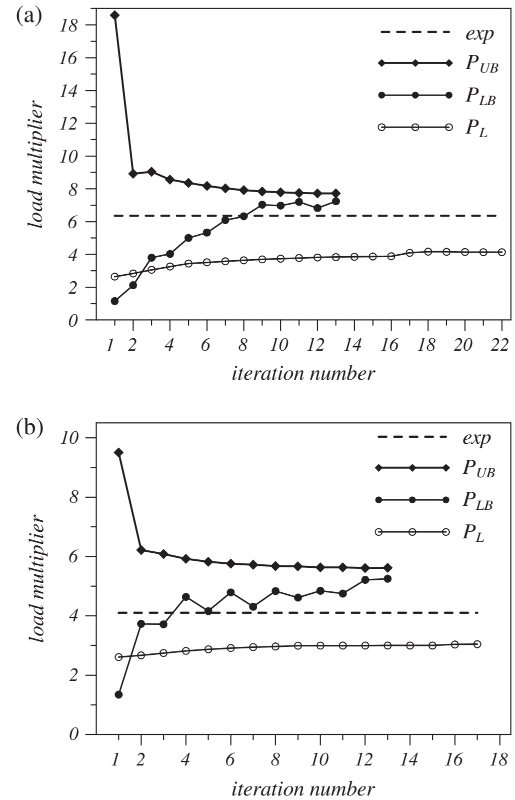

Fig. 7. Values of the upper (P_{UB}) and lower bounds (P_{LB} and P_L) to the collapse load multiplier versus iteration number; numerical results (solid lines with symbols) against collapse experimental treshold (dashed lines) for: (a) specimen #3; (b) specimen #4.

quite good for tests #1 and #2 of the examined joint. The ECM, used to evaluate the lower bound P_L, seems to be more, perhaps too much, conservative requiring sometimes several analyses to attain the final "compensated" value as shown in Fig. 6b. Nevertheless, the results obtained for tests #3 and #4 clearly show that the P_{LB} (lower bound computed via LMM), being actually a lower bound to the least upper bound (see also Remark 5 at Section 3.2), *might be above* the experimentally detected collapse load multiplier, as shown in Fig. 7a and b. For these tests indeed the P_L value appears to be the only significative for design purposes. Far from giving a definitive direction, but grounding on the results obtained for the examined problem, a possible design methodology, oriented to estimate the load bearing capacity of a pinned-joint composite plate, seems to be the one which evaluates an upper and a lower bound to the collapse load; the former via the LMM, the latter via the ECM.

In all cases a monotonic rapid convergence of the P_{UB} sequence is observed as expected by the present LMM, see Remark 1 at Section 4.1. It is worth to say that the good performance of the proposed approach, confirmed in many of the run tests, drastically reduces when three-dimensional or through-thickness effects play a major role in the mechanical behaviour of the specimen. Such effects are obviously not considered with the present 2D formulation. Indeed, the same values of σ_{BRU} obtained for prototypes having the same W/D and E/D ratios but with different thickness are consistent with the 2D FE analysis but contradict the experimental evidences. To this concern it is to observe that a different thickness implies a different stacking sequence of the laminate layers that can affect the mechanical characteristics of the laminate. To the authors' opinion a good strategy could be a LMM applied *layer-by-layer*, i.e. by using multilayer FEs so carrying out the matching taking into account the stacking sequence of the specimen. The use of multilayer FEs should give some benefits also to the stress redistribution procedure of the EC approach. Another essential need is to test, for each prototype, a statistically more significative number of specimens.

Two further comments concern the ECM here employed; precisely, with reference to the plots of Fig. 8a and b pertinent to specimen #1, the following can be observed. The sequences of elastic analyses carried on for the P_L evaluation can be repeated at increasing load levels $P_D \cdot P$ (P = 1 kN) obtaining, as observed by who conceived the method, increasing values of the lower bound approaching the collapse load multiplier; see Fig. 8a where the P_L values for three different design loads are plotted. Small further increases of P_D can however require a very high number of further iterations (that is of elastic analyses of the specimen) to attain a "compensated" admissible solution so reducing the competitiveness of the direct method with respect to a step-by-step elasto-plastic FE analysis. On the other hand, as shown in Fig. 8b, the use of a squared updating ratio as the one proposed in Eq. (14) seems to improve considerably the convergence rate.

5.2. The ultimate behaviour: collapse mechanisms

As observed in Section 2, the prediction of the collapse mechanism of the joint is undoubtedly a crucial goal. In Figs. 9a and b, 10a and b and 11a and b are plotted the collapse mechanisms predicted by the LMM for specimens #1, #2 and #3 respectively. The mechanisms are here individuated by the band plots, at last iteration, of the node displacement components. In particular: Fig. 9a and b show *net tension* failure mode, Fig. 10a and b a combined *bearing/shear-out* failure mode and Fig. 11a and b a *bearing* failure

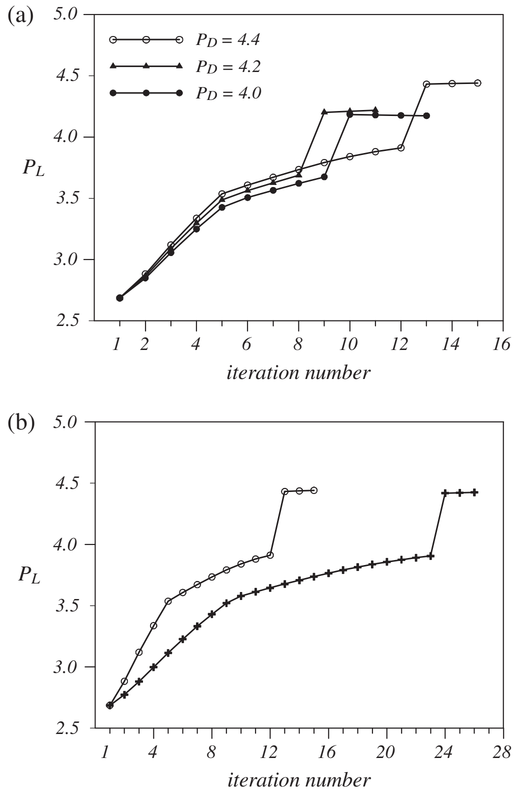

Fig. 8. Values of the lower bound P_L to the collapse load multiplier versus iteration number for specimen #1: (a) results obtained for three different design load $P_D \cdot P$; (b) P_L sequences obtained with a squared updating ratio as in Eq. (14) (solid line with noughts) and values of P_L without squared ratio (solid line with crosses).

mode, all in agreement with the experimental observed modes reported in Table 3 for the run examples. These results are obviously very encouraging also for the pretty good definition of the collapse zone.

6. Concluding remarks and future research

A typical problem of composite structural elements such as the evaluation of the strength as well as the prediction of the failure mechanism of joints between composite plates has been addressed. The problem has been treated in a simplified manner that is in terms of evaluation of an *upper* and a *lower bound* to the *collapse (failure) load multiplier*. An approach based on *limit analysis theory* has been proposed.

From a wider point of view, the expounded approach concerns limit analysis of a class of anisotropic structures made of a material whose constitutive behaviour can be governed by a yield criterion expressed by a quadratic (strictly convex) stress function. In the present study the material obeys, by hypothesis, to a Tsai–Wu type yield condition, defined as a second-order tensor polynomial form of the Tsai–Wu failure criterion for composite laminates in plane stress conditions. The lack of associativity, here overcome by a non standard limit analysis approach, makes impossible the definition of a collapse load multiplier and obliges to search for an upper and a lower bound to it. The knowledge of such bounds as well as the evaluation of the gap between them is obviously essential for design purposes.

The above upper and lower bounds to the collapse load have been evaluated via two well known numerical procedures for limit analysis which also share common roots, namely: the *Linear Matching Method* and the *Elastic Compensation Method*. Both procedures have been adapted to the assumed yield condition introducing some novelties. The former, rephrased in a dimensionless stress space, gives rise to an iterative scheme furnishing, at each iteration, a lower and an upper bound to the limit load multiplier. The latter, here devoted to a lower bound evaluation, has been formulated in terms of stress vectors suggesting some changes which seem to improve the convergence rate. The two procedures make use of sequences of elastic analyses so resulting easy to handle via any commercial finite element code suitably driven by an home-made subroutine (here implemented in Fortran).

A pin-loaded plate, under plane stress conditions, has been analyzed and the obtained results have been compared with few experimental ones get from the literature. The numerical findings, at least for the examined problem, are quite promising showing the potentialities of the proposed methodology and its competitiveness with respect to a burdensome step-by-step nonlinear analysis. An effective strategy for design purposes seems the one which evaluates an upper bound via the LMM and a lower bound via the ECM, such choice exhibits, at least in the run examples, a good ability of bracketing the collapse load value detected via laboratory tests. Moreover, the results obtained in terms of collapse mode prediction of the analyzed prototypes are indeed very encouraging either for the very good agreement with the experimental findings or for the accurate localization of the collapse zone.

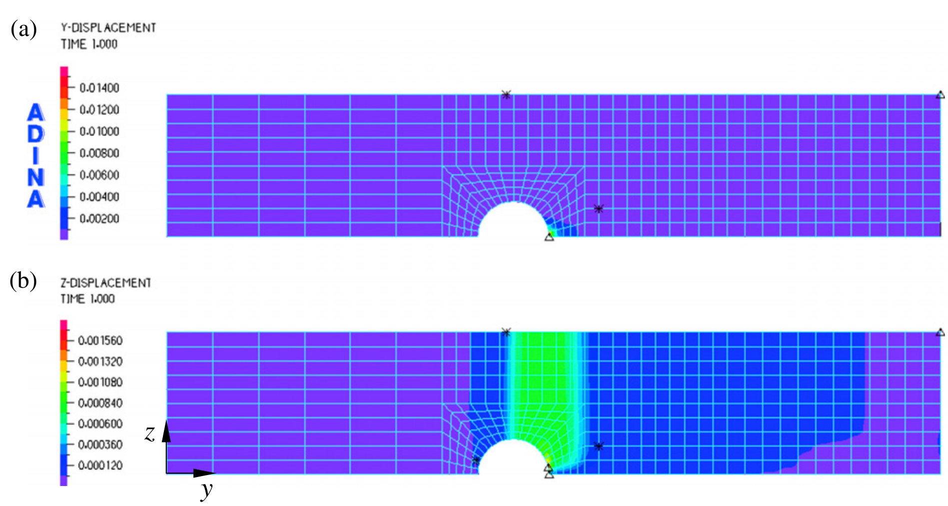

Fig. 9. Pin-loaded plate of Fig. 1, collapse mechanism of net-tension type for specimen #1: (a) y-displacements; (b) z-displacements.

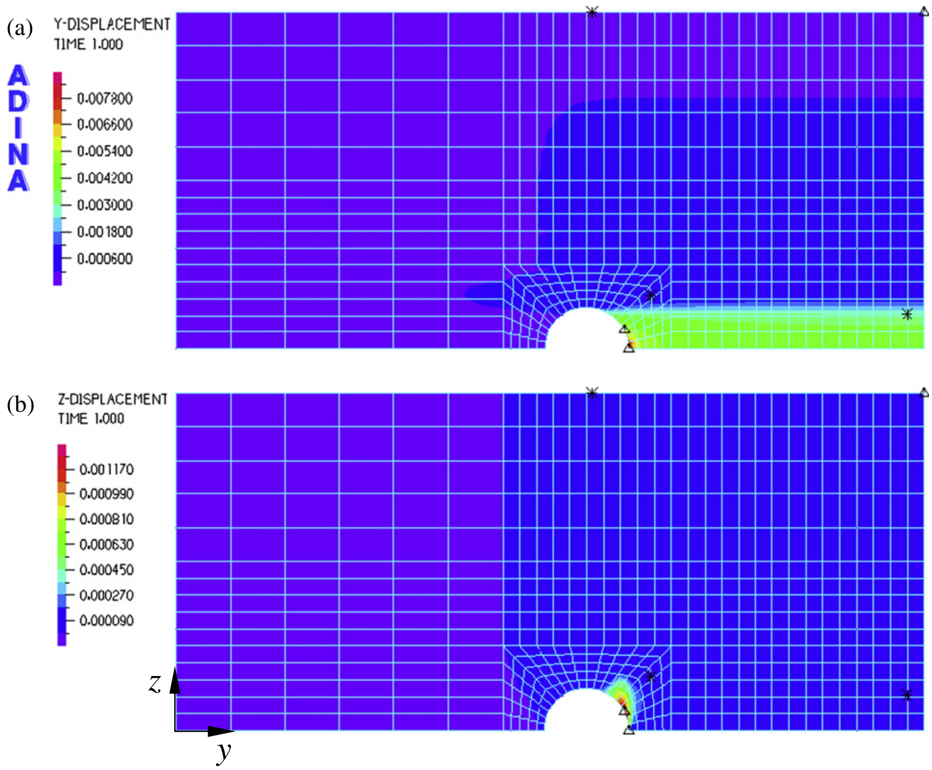

Fig. 10. Pin-loaded plate of Fig. 1, collapse mechanism of bearing/shear-out type for specimen #2: (a) *y*-displacements; (b) *z*-displacements.

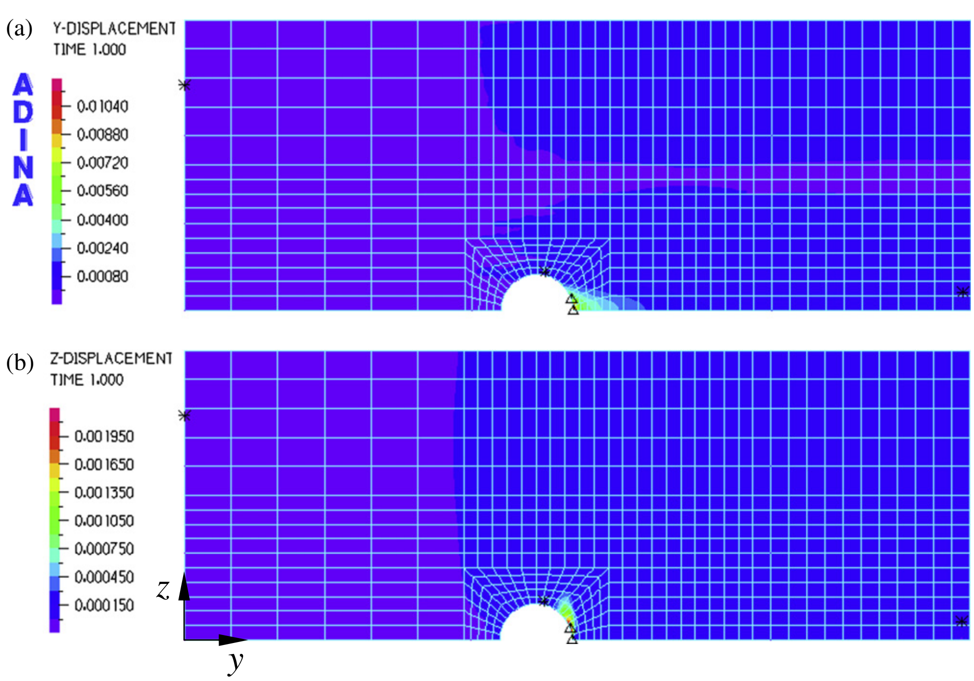

Fig. 11. Pin-loaded plate of Fig. 1, collapse mechanism of bearing type for specimen #3: (a) *y*-displacements; (b) *z*-displacements.

Some numerical findings show the need of investigations to take into account three-dimensional effects revealed by the experimental evidences and here disregarded by a 2D FE formulation. Further studies are certainly needed; a parametric analysis or an incremental elasto-plastic analysis could be performed to investigate the influence of manufacturing and testing process of the specimens or to get alternative numerical findings. A possible future step forward could also be a better FE-modeling of the composite laminate whose mechanical characteristics can be affected by the stacking sequence of the fiber layers. The idea is to make use of multilayer 2D elements so performing the expounded numerical procedures at the layer prototype level. Another crucial task is the definition of apposite experimental tests on prototypes suffering the same load conditions, but having different geometry and/or fabricated with a different manufacturing technology. To the authors' opinion, the full reliability on a methodology as the one here proposed can be achieved only by comparison with a statistically meaningful number of experimental results. These are, at present, the main targets of an ongoing research work being this study just a first, but not trivial, step for the numerical limit analysis of mechanically fastened joints in composite laminates.

Acknowledgement

The financial support of the Italian Ministero dell'Università e della Ricerca (MiUR) is gratefully acknowledged.

References

[1] ADINA R & D, Inc. Theory and modeling guide. Watertown (MA, USA): Adina R & D; 2002.
[2] Andersen KD, Christiansen E, Overton ML. Computing limit loads by minimizing a sum of norms. SIAM J Sci Comput 1988;19:1046–62.
[3] Ascione F, Feo L, Maceri F. An experimental investigation on the bearing failure load of glass fibre/epoxy laminates. Compos Part B: Eng 2009;40:197–205.
[4] Ascione F, Feo L, Maceri F. On the pin-bearing failure load of GFRP bolted laminates: an experimental analysis on the influence of bolt diameter. Compos Part B: Eng 2010;41:482–90.
[5] Atkinson JH, Potts DM. Stability of a shallow circular tunnel in cohesionless soil. Géotechnique 1977;27:203–15.
[6] Barrera O, Cocks ACF, Ponter ARS. Evaluation of the convergent properties of the Linear Matching Method for computing the collapse of structural components. Eur J Mech A: Solids 2009;28:655–67.
[7] Belytschko T, Hodge PG. Plane stress limit analysis by finite elements. J Eng Mech Div 1970;96:931–43.
[8] Boulbibane M, Ponter ARS. Extension of the linear matching method to geotechnical problems. Comput Methods Appl Mech Eng 2005;194:4633–50.
[9] Camanho PP, Lambert M. A design methodology for mechanically fastened joints in laminated composite materials. Compos Sci Technol 2006;66:3004–20.
[10] Camanho PP, Matthews FL. Stress analysis and strength prediction of mechanically fastened joints in FRP: a review. Composites Part A 1997:529–47.
[11] Capsoni A, Corradi L, Vena P. Limit analysis of anisotropic structures based on the kinematic theorem. Int J Plasticity 2001;17:1531–49.
[12] Chen S, Liu Y, Cen Z. Lower bound limit analysis by using EFG method and nonlinear programming. Int J Numer Methods Eng 2008;74:391–415.
[13] Chen L, Liu Y, Yang P, Cen Z. Limit analysis of structures containing flaws based on a modified elastic compensation method. Eur J Mech A: Solids 2008;27:195–209.
[14] Chen HF, Ponter ARS, Ainsworth RA. The linear matching method applied to the high temperature life integrity of structures. Part. 1. Assessment involving constant residual stress fields. Int J Press Ves Piping 2006;83:123–35.
[15] Chen HF, Shu DW. A numerical method for lower bound limit analysis of 3-D structures with multi-loading systems. Int J Press Ves Piping 1999;76:105–12.
[16] Corradi L, Vena P. Limit analysis of orthotropic plates. Int J Plasticity 2003;19:1543–66.
[17] D5961/D5961M-05. Standard test method for bearing response of polymer–matrix composite laminates. Composite materials. West Conshohocken (PA): ASTM International; 2005. p. 15.03.
[18] Dhalla AK, Jones GL. ASME code classification of pipe stresses: a simplified elatic procedure. Int J Press Ves Piping 1986;26:145–66.
[19] Drucker DC, Prager W, Greenberg HJ. Extended limit design theorems for continuos media. Quart Appl Math 1952;9:381–9.
[20] Drucker DC, Prager W. Soil mechanics and plastic analysis or limit design. Quart Appl Math 1952;10:157–65.
[21] Francescato P, Pastor J. Lower and upper numerical bounds to the off-axis strength of unidirectional fiber-reinforced composite by limit analysis method. Eur J Mech A: Solids 1997;16:213–34.
[22] Fuschi P, Pisano AA, Barrera O. Limit analysis of orthotropic laminates by Linear Matching Method. In: Weichert D, Ponter ARS, editors. Limit states of materials and structures – direct methods. Wien: Springer; 2009. p. 197–220.
[23] Gray PJ, McCarthy CT. A global bolted joint model for finite element analysis of load distributions in multi-bolt composite joints. Compos Part B: Eng 2010;41:317–25.
[24] Hamilton R, Boyle JT. Simplified lower bound limit analysis of transversely loaded thin plates using generalised yield criteria. Thin-Walled Struct 2002;40:503–22.
[25] Hamilton R, Boyle JT, Shi J, Mackenzie D. A simple upper bound method of calculating approximate shakedown loads. Trans ASME J Press Ves Technol 1998;120:195–9.
[26] Heyman J. The stone skeleton. Int J Solids Struct 1966;2:249–79.
[27] Hodge PG, Belytschko T. Numerical methods for the limit analysis of plates. Trans ASME J Appl Mech 1968;35:796–802.
[28] Jones RM. Mechanics of composite materials. 2nd ed. Philadelphia (PA, USA): Taylor & Francis Inc.; 1999.
[29] Josselin de Jong G. Lower bound collapse theorem and lack of normality of strain rate to yield surface of soils. In: Rheology and soil mechanics: IUTAM Symposium, Grenoble, 1964. Berlin (Germany): Springer-Verlag; 1966.
[30] Kooharian A. Limit analysis of voussoir and concrete arches. J Am Concr Inst 1952;24:317–28.
[31] Li HX, Yu HS. Limit analysis of composite materials based on an ellipsoid yield criterion. Int J Plasticity 2006;22:1962–87.
[32] Lopez RH, Luersen MA, Cursi ES. Optimization of laminated composites considering different failure criteria. Compos Part B: Eng 2009;40:731–40.
[33] Lyamin AV, Sloan SW. Lower bound limit analysis using linear programming. Int J Numer Methods Eng 2002;55:573–611.
[34] Lubliner J. Plasticity theory. New York: Macmillan Pub. Co.; 1990.
[35] Ma G, Gama BA, Gillespie Jr JW. Plastic limit analysis of cylindrically orthotropic circular plates. Compos Struct 2002;55:455–66.
[36] Mackenzie D, Boyle JT. A method of estimating limit loads by iterative elastic analysis. Parts I, II, III. Int J Press Ves Piping 1993;53:77–142.
[37] Makrodimopoulos A, Martin CM. Lower bound limit analysis of cohesive-frictional materials using second-order cone programming. Int J Numer Methods Eng 2006;66:604–34.
[38] Marriot DL. Evaluation of deformation or load control of stresses under inelastic conditions using elastic finite element stress analysis. In: Proc. ASME PVP conference, 136 Pittsburg; 1988.
[39] McLaughlin Jr PV, Batterman SC. Limit behaviour of fibrous materials. Int J Solids Struct 1970;6:1357–76.
[40] Muñoz JJ, Bonet J, Huerta A, Peraire J. Upper and lower bounds in limit analysis: adaptive meshing strategies and discontinuous loading. Int J Numer Methods Eng 2008. doi:10.1002/nme. 2421.
[41] Palmer AC. A limit theorem for materials with non-associated flow laws. J Mécanique 1966;5:217–22.
[42] Pisano AA, Fuschi P. A numerical approach for limit analysis of orthotropic composite laminates. Int J Numer Methods Eng 2007;70:71–93.
[43] Ponter ARS, Carter KF. Limit state solutions, based upon linear elastic solutions with spatially varying elastic modulus. Comput Methods Appl Mech Eng 1997;140:237–58.
[44] Ponter ARS, Fuschi P, Engelhardt M. Limit analysis for a general class of yield conditions. Eur J Mech A: Solids 2000;19:401–21.
[45] Prager W. An introduction to plasticity. Reading (MA): Addison-Wesley; 1959.
[46] Radenkovic D. Théorèmes limites pour un materiau de Coulomb à dilatation non standardisée. CR Acad Sci Paris 1961;252:4103–4.
[47] Save M. Atlas of limit loads of metal plates, shells and disks. Amsterdam: Elsevier; 1995.
[48] Seshadri R. The effect of multiaxiality and follow-up on creep damage. J Press Ves Technol 1990;112:378–85.
[49] Seshadri R. Simplified methods for determining multiaxial relaxation and creep damage. In: ASME PVP, San Diego, vol. 210–2; 1991. p. 173–80.
[50] Seshadri R. The generalised local stress strain (GLOSS) analysis – theory & applications. Journal Pressure Vessel Technology 1991:219–27 [25th anniversary volume].
[51] Seshadri R, Fernando CPD. Limit loads of mechanical components and structures using the GLOSS R-Node method. In: ASME PVP, San Diego, vol. 210–2; 1991. p. 125–34.
[52] Shield RT. On Coulomb's law of failure in soils. J Mech Phys Solids 1955;4:10–6.
[53] Shu LS, Rosen BW. Strength of fiber-reinforced composites by limit analysis methods. J Compos Mater 1967;1:366–81.
[54] Sloan SW. Lower bound limit analysis using finite elements and linear programming. Int J Numer Anal Methods Geomech 1988;12:61–77.
[55] Sloan SW, Kleeman PW. Upper bound limit analysis using discontinuous velocity fields. Comput Methods Appl Mech Eng 1995;127:293–314.
[56] Soden PD, Kaddour AS, Hinton MJ. Recommendations for designer and researchers resulting from the word-wide failure exercise. Compos Sci Technol 2004;64:589–604.
[57] Thoppul SD, Finegan J, Gibson RF. Mechanics of mechanically fastened joints in polymer–matrix composite structures – a review. Compos Sci Technol 2009;69:301–29.
[58] Tsai SW, Hann HT. Introduction to composite materials. Westport (CT, USA): Technomic Pub. Co.; 1980.
[59] Tsai SW, Wu EM. A general theory of strength for anisotropic materials. J Compos Mater 1971;5:58–80.
[60] Weichert D, Ponter ARS, editors. Limit states of materials and structures – direct methods. Springer; 2009.
[61] Wu TJ, Hahn HT. The bearing strength of e-glass/vinyl–ester composites fabricated by VARTM. Compos Sci Technol 1998;58:1519–29.
[62] Yu HS, Sloan SW. Finite element limit analysis of reinforced soils. Comput Struct 1997;63:567–77.
[63] Zhang H, Liu Y, Xu B. Plastic limit analysis of ductile composite structures from micro- to macro-mechanical analysis. Acta Mech Solida Sinica 2009;22(1):73–84.
[64] Zhang X, Liu Y, Zhao Y, Cen Z. Lower bound limit analysis by the symmetric Galerkin boundary element method and the complex method. Comput Methods Appl Mech Eng 2002;191:1967–82.
[65] Zheng X, Booker JR, Carter JP. Limit analysis of the bearing capacity of fissured materials. Int J Solids Struct 2000;37:1211–43.